Notes on the Barkas-Andersen effect

Sigmund, Peter; Schinner, Andreas

Published in:
European Physical Journal D. Atomic, Molecular, Optical and Plasma Physics

Publication date:
2014

Document version
Submitted manuscript

Citation for pulished version (APA):
Sigmund, P., & Schinner, A. (2014). Notes on the Barkas-Andersen effect. European Physical Journal D. Atomic, Molecular, Optical and Plasma Physics, 68, 318-325.

EPJ manuscript No.
(will be inserted by the editor)

Notes on Barkas-Andersen Effect

Peter Sigmund[1] and Andreas Schinner[2]

[1] Department of Physics, Chemistry and Pharmacy, University of Southern Denmark, DK-5230 Odense M, Denmark
[2] Institut für Experimentalphysik, Johannes Kepler Universität, A-4040 Linz-Auhof, Austria

the date of receipt and acceptance should be inserted later

Abstract. Stimulated by recent statements in the literature on electronic stopping of heavy ions in matter, we try to clarify some central theoretical aspects of the Barkas-Andersen effect, about which there does not seem to be unanimous agreement in the community. We address the role of inner versus outer target shells, of projectile screening by bound electrons, the interference between Lindhard's description and perturbation theory, as well as the equivalence between a single-electron versus Fermi-gas description of the effect.

PACS. 34.50.Bw; Energy loss and stopping power and 61.85.+p; Channeling phenomena and 52.40.Mj; Particle beam interactions in plasma

1 Introduction

The Barkas-Andersen effect denotes two observations in experimental studies of the stopping of swift charged particles in matter,

- Barkas and coworkers [1–3] observed that the stopping cross section for a positively charged particle can be greater than that for the equivalent antiparticle, denoted as *Barkas splitting* in the following, and
- Andersen and coworkers [4–6] observed a velocity-dependent deviation from strict square dependence of the stopping cross section for light ions on their atomic number Z_1, denoted as *Barkas-Andersen correction* in the following.

The tight connection between these two observations was demonstrated experimentally in studies of the stopping of swift antiprotons [7–9].

These observations have generated a rich theoretical literature, initiated by Ritchie and coworkers [10], with highlights summarized in ref. [11].

The effect was quantified originally [4] in terms of a contribution $\propto Z_1^3$ to the Bethe [12] stopping formula, where $Z_1 e$ is the charge of the projectile. After the recognition [13] and experimental verification [5,6] of the presence of higher-order Z_1 contributions, it has become customary to quantify the effect by a Barkas ratio

$$R = \frac{S^+ - S^-}{S^+ + S^-}, \tag{1}$$

where S^+ denotes the stopping cross section of a material for protons and S^- for antiprotons, and similarly for other particle-antiparticle pairs. Here

$$\Delta S = (S^+ - S^-)/2 \tag{2}$$

denotes the sum of all terms proportional to an odd power in Z_1 contributing to the stopping cross section, whereas

$$S_0 = (S^+ + S^-)/2 \tag{3}$$

represents the sum of all even powers of Z_1. In other words, R denotes the relative deviation of the stopping cross section for protons from the mean value S_0 which could be represented by the Bethe stopping formula or one of its extensions [11].

Measurements by Andersen et al. [4] showed that the leading correction is proportional to Z_1^3 and decreasing with increasing projectile speed. This was confirmed in calculations by Ashley et al. [10] and Lindhard [13], who found that the quantity

$$\frac{1}{\xi} = \frac{Z_1 e^2 \omega}{m v^3} \tag{4}$$

is the appropriate scaling variable for this effect. Here ω is a characteristic resonance frequency of an atom in the stopping medium and $\xi = mv^3/Z_1 e^2 \omega$ the scaling variable in classical Bohr stopping theory [14]. The very fact of the occurrence of this variable – which does not contain $\hbar$ – led Lindhard [13] to the conclusion that we deal with a classical effect.

Several calculations, starting with [13, 15], confirmed that $1/\xi$ plays an analogous role in a Fermi gas, with ω in eq. (4) being replaced by the plasma frequency ω_P.

2 Problems Addressed

The present paper has been stimulated by recent studies of the topic which left open some important questions and/or

led to questionable conclusions. We address the following items:

1. What is the relation between Lindhard's description [13] of the Barkas-Andersen effect and the description by Ashley et al. [10]?
2. Is a free-electron-gas description of the effect equivalent with a description in terms of an ion-atom interaction?
3. Is there a physical meaning to talking about a Barkas effect for dressed ions?

Although our conclusions differ in several respects from assumptions underlying much of the existing literature, we find it likely that in part of these cases the above questions have not been asked. Therefore, we quote key references when there is a specific reason but do not aim at a complete bibliography.

3 Binding versus Screening

Bohr's classical stopping theory [14] addresses the interaction of a point charge $Z_1 e$ with an electron that is bound harmonically to a nucleus with a resonance frequency ω. The mean energy loss is determined by the stopping cross section

$$S(v) = \int 2\pi p\, dp\, T(p), \tag{5}$$

where p and $T(p)$ denote the impact parameter and energy loss in an ion-electron collision, respectively. Ashley et al. [10], viewing the Barkas-Andersen effect as a deviation from the leading order in a perturbation expansion of the energy loss *in powers of* Z_1, wrote $T(p)$ in the form

$$T(p) = T^{(2)}(p) + T^{(3)}(p) \ldots, \tag{6}$$

where $T^{(n)}(p)$ is proportional to Z_1^n. Expressions for $T^{(2)}(p)$ are standard textbook material [11]. $T^{(3)}(p)$ was evaluated following Bohr's [14] procedure to calculate $T^{(2)}(p)$. This involves a multipole expansion which is valid only for 'distant' collisions. It was found that the ratio $T^{(3)}(p)/T^{(2)}(p)$ is proportional to the factor $1/\xi$, eq. (4).

Hill and Merzbacher [16] demonstrated that the result of Ashley et al. [10] also emerged from quantal instead of classical perturbation theory.

Lindhard [13] started from the well-known fact that the differential cross section for Coulomb scattering is strictly proportional to Z_1^2. The presence of the factor ω in $1/\xi$ was interpreted as a deviation from free-Coulomb scattering. From Bohr's work it is known that collisions are free-Coulomb-like for impact parameters well below the adiabatic radius v/ω, and increasingly screened at larger impact parameters. By introducing a screened ion-electron interaction potential

$$V_{\rm eff}(r) = -\frac{Z_1 e^2}{r} e^{-r/a} \tag{7}$$

with $a \propto v/\omega$, Lindhard was able to derive an expression for the Barkas-Andersen correction about twice the size of the one found by Ashley et al. Most important, eq. (7) did not enforce a split between close and distant collisions.

The subsequent discussion of the validity of Lindhard's approach has been extensive and has generated numerous experimental and theoretical studies, a concise survey of which has been given in ref. [11]. While the validity of the approach has gradually been accepted, it is not clear whether, as implied by Lindhard, his approach covers the complete phenomenon or, as implied recently [17–19], that one deals with two independent mechanisms, one for distant collisions found by Ashley et al, and another one for close collisions found by Lindhard. This aspect will be studied here by comparing the distant-collision limit of Lindhard's approach to that of Ashley et al.

We have carried out Lindhard's procedure without resorting to a perturbation expansion [20] by evaluating the classical scattering integral for the potential (7) numerically. We found that with the choice of

$$a = \frac{v}{\omega} \tag{8}$$

we could reproduce the lowest-order term of the kinetic-energy transfer,

$$T^{(2)}_{\rm kin}(p) = \frac{2mv^2}{\xi^2} \times \left[K_1\left(\frac{\omega p}{v}\right)\right]^2 \tag{9}$$

rigorously for large impact parameters, where $K_1(\zeta)$ is a modified Bessel function in standard notation [21].

In Bohr theory, energy is also transferred to potential energy of the harmonic-oscillator atom. While potential-energy transfer does not take place in a free elastic ion-electron collision, regardless of the interaction potential, we were able to show in ref. [20] that by invoking angular momentum transfer, this contribution takes the form

$$T^{(2)}_{\rm pot}(p) = \frac{2mv^2}{\xi^2} \times \left[K_0\left(\frac{\omega p}{v}\right)\right]^2 \tag{10}$$

in the distant-collision limit [20], in complete agreement with Bohr's result [14].

Rather than following either Ashley et al. or Lindhard and going to the next order order in Z_1, we evaluated kinetic and potential energy loss without recurrence to a series expansion and thus obtained Barkas-Andersen corrections at velocities down to well below the limit of validity of a Z_1^3 correction [20,22]. We obtained good agreement with experiments [23].

For the present purpose, however, we need to determine third-order terms corresponding to eqs. (9) and (10). This is easily done by means of the perturbation expansion of the classical scattering integral as well as the time integral following a procedure developed by Lehmann and Leibfried [24] and described in ref. [11]. The resulting integrals are elementary and yield

$$T^{(3)}_{\rm kin}(p) = \frac{2mv^2}{\xi^3} \times 4K_1\left(\frac{\omega p}{v}\right) K_1\left(2\frac{\omega p}{v}\right), \tag{11}$$

$$T^{(3)}_{\rm pot}(p) = \frac{2mv^2}{\xi^3} \times 6K_0\left(\frac{\omega p}{v}\right) K_0\left(2\frac{\omega p}{v}\right). \tag{12}$$

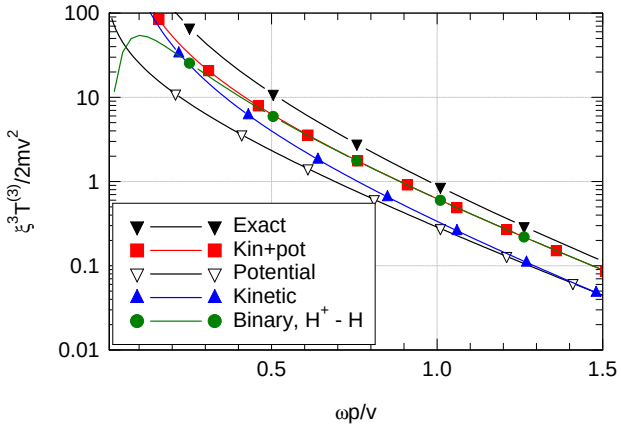

Fig. 1. Leading Barkas-Andersen correction $\propto Z_1^3$: Exact: from [25], equivalent with [10]; kinetic: eq. (11); potential: eq. (12); binary: Sum of odd terms in Z_1 according to binary stopping theory [20].

Figure 1 shows $T^{(3)}_{\rm kin}(p)$ and $T^{(3)}_{\rm pot}(p)$ in a universal plot as well as the sum of the two, compared with the exact Z_1^3 correction for a classical harmonic oscillator [10], reevaluated according to ref. [25]. Also included is a curve labeled 'binary', which represents a nonperturbative Barkas-Andersen correction according to binary stopping theory [20]. The latter curve has been included to illustrate the limitations of the Z_1^3 approximation. It is seen that for $\omega p/v > 1$ the error is invisible in the graph, and even for $\omega p/v = 1/2$ it is only 5 %.

With this, we may conclude as follows on the first of the three questions formulated above:

- There is general agreement that the treatment by Ashley et al. is incomplete since it ignores Barkas splitting in close collisions, the existence of which is well documented.
- Lindhard's derivation implies that his treatment covers close and distant collisions, although it is not meant to be quantitative [1].
- Figure 1 demonstrates that Lindhard's procedure, when amended by a potential-energy transfer according to binary theory ('kin+pot') yields a result slightly smaller than the exact one.
- Following Lindhard, one could try to change this estimate by modifying the screening radius, adopting another functional shape of the potential and/or allowing for a deviation from spherical symmetry. Lindhard's modification was dictated by electron-gas arguments. For an ion-atom interaction, we do not find it justified to operate with different screening radii in subsequent orders of a perturbation expansion.
- If only the kinetic-energy transfer is considered, as was done in ref. [17], the result deviates by more than a factor of two from the exact one over the entire range of validity of the first-order perturbation.

[1] 'I will try to show that the theory is quite simple basically, but this does not mean that I am sure of all details of it' [13].

In other words, Lindhard's approach to the Barkas-Andersen effect, when carried out with an exponential screening function, underestimates the distant-collision limit of Ashley et al. by up to a factor of two for $\omega p/v \gtrsim 1/2$, if potential-energy transfer is included, although the difference decreases to ~ 20 % at $\omega p/v \simeq 1.5$.

If potential-energy transfer is left out of consideration, the discrepancy exceeds a factor of two over the entire range of impact parameters. Although this feature is not mentioned in ref. [17], it may be the reason why Lindhard's procedure has been considered to concern only close collisions [17–19].

While there is equipartition between kinetic and potential energy transfer at large impact parameters in the lowest (Bohr) order, potential-energy transfer dominates by a factor of 6/4 in the next order according to eq. (11) and (12). This, however, happens at impact parameters that are insignificant in the evaluation of the stopping cross section.

4 Electron Gas

There is a large followup literature on the earliest studies of the Barkas effect in the Fermi gas [13, 15, 26]. In the present context, the only issue to be discussed is whether or not a description in terms of single-particle scattering on a potential of the type of eq. (7) can produce a valid estimate of the Barkas-Andersen effect for distant interactions.

Unlike in the previous section, transfer of potential energy is not an issue for an electron-gas target. On the other hand, distant interactions refer to small momentum transfers and are typically of a collective nature. It is, therefore, by no means obvious that a single-particle description could be adequate. Instead of looking at differential energy transfers, as was done in the previous section, we here look at the stopping cross section. It is well-known from Bohr, Bethe and Lindhard theory [12,14,27,28] that there is a rough equipartition between contributions from close and distant collisions to the stopping cross section in the lowest order in Z_1. Our adopted criterion for a positive answer will be, therefore, the ability of the model to produce a stopping cross section in the lowest order of the right magnitude and energy dependence.

The reference standard here is the stopping cross section per target electron,

$$S = \frac{4\pi Z_1^2 e^4}{mv^2} \ln \frac{2mv^2}{\hbar\omega_P} \qquad (13)$$

according to [29] and confirmed in refs. [27, 28]. Here, ω_P is the classical plasma frequency. Shell and relativistic corrections are ignored.

Since eq. (13) is a quantum formula, the proper perturbation scheme to treat scattering on the potential (7) is the first Born approximation which leads to a differential cross section

$$d\sigma(v,\Theta) = \left(\frac{Z_1 e^2}{2mv^2}\right)^2 \frac{2\pi \sin\Theta\, d\Theta}{\left[\sin^2(\Theta/2) + (\hbar/2mva)^2\right]^2}. \qquad (14)$$

and a stopping cross section

$$S = \frac{4\pi Z_1^2 e^4}{mv^2}\left\{\frac{1}{2}\ln\left[1+\left(\frac{2mva}{\hbar}\right)^2\right] - \frac{1}{1+(\hbar/2mva)^2}\right\} \tag{15}$$

according to Arista [30]. For $2mva/\hbar \gg 1$ this reduces to

$$S = \frac{4\pi Z_1^2 e^4}{mv^2}\left(\ln\frac{2mva}{\hbar} - \frac{1}{2}\right); \tag{16}$$

If we insert

$$a = v/\omega_P, \tag{17}$$

this agrees with eq. (13), except for the term -1/2 in the brackets. Now, the same error occurs in the stopping cross section of an atom in Bohr stopping theory if potential-energy transfer, expressed by eq. (10), is left out in the integration, as was demonstrated in ref. [31]. We therefore assert that this is the error made when the stopping cross section in the leading order is determined by the kinetic-energy transfer in collisions with individual electrons.

In finding an estimate for the Barkas-Andersen effect, Lindhard [13] applied a screening radius

$$a = \frac{2}{\pi}\frac{v}{\omega}, \tag{18}$$

i.e., a value smaller than (17). An explanation for this choice was given in ref. [17], which makes it explicit that this value refers to the screening in close collisions. This is actually the point where Arista et al. [17] explicitly refer to the work of Ashley et al. [10] as a separate effect.

We find it difficult to argue for different screening radii in first and second order perturbation theory. In fact, we see no compelling evidence in favor of the application of eq. (18) in the present context. A definite answer might be found from a rigorous evaluation of the next order in analogy to the calculation leading to eq. (11). Rather than going into second-order Born approximation we prefer to make reference to Esbensen and one of us [32], where the energy loss of a point charge in a harmonic-oscillator gas was analysed. Here it was found that a key role is played by the quantity

$$\alpha_0 = \sqrt{\omega_0^2 + \omega_P^2}, \tag{19}$$

where ω_0 is the oscillator frequency and ω_P the plasma frequency. The difference in the distributions of differential energy-loss per target electron between an electron gas ($\omega_0 = 0$) and an isolated oscillator ($\omega_P = 0$) turned out to be less than 10 %, and the same was found true for the stopping number.

Considering the basically classical nature of the Barkas-Andersen effect we refrain from going into detailed quantal treatments such as [26, 33–35] and conclude as follows:

- Despite significant differences in the physical situation, there is a well-established analogy between the stopping properties of a classical or quantal electron gas and an isolated atom, in particular an atom modeled as a harmonic oscillator.
- We do not find evidence that this analogy is less far-going in the third than in the second order in Z_1.

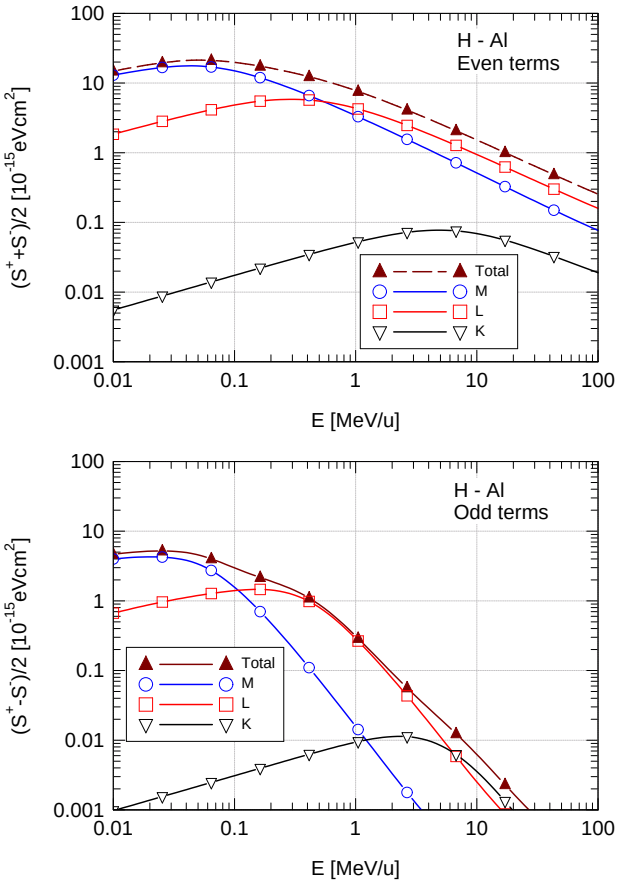

Fig. 2. Even (top) and odd (bottom) terms making up the stopping cross section of aluminium for bare protons according to binary stopping theory. See text.

5 Role of Inner Shells

In view of the leading role of the factor $1/\xi$, the non-relativistic Barkas-Andersen effect tends to be most pronounced at fairly low beam velocities. At the same time, the factor $1/\xi$ is proportional to ω, i.e., it must increase from outer to inner target shells. On the other hand, the contribution of inner shells to the stopping cross section of a target atom tends to decrease with decreasing beam velocity because of shell and binding corrections. Thus, the relative contributions of various shells to the stopping cross section cannot be expected to reflect the magnitude of the Barkas-Andersen effect.

Here we study the case of hydrogen ions in aluminium. Calculations are performed by the PASS code [36] implementing binary stopping theory [20]. Stopping cross sections are determined for bare protons and bare antiprotons incident on solid aluminium, and even and odd terms are extracted via eqs. (2) and (3), respectively. Input parameters are taken from ref. [37]. We operate with three target shells, where the M shell is treated as a free electron gas.

Figure 2 shows results for bare protons in aluminium. The upper graph demonstrates the well-known fact that the stopping cross section at low projectile speed – here $\lesssim 100$ keV – is almost exclusively determined by the outer-

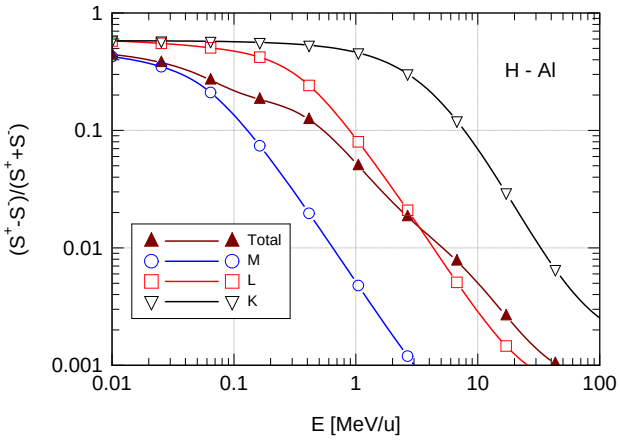

Fig. 3. Barkas ratio R, eq. (1), for H in Al, separated into three shells and total, according to binary stopping theory.

most electrons. At high velocities, the contributions from various shells come closer to reflecting the number of electrons occupying those shells.

In the bottom graph, the relative magnitude of the four contributions is more or less inverted at high energies, although their contribution falls below the 1 % level at $\gtrsim 10$ MeV. The most prominent change is the dominating role of the innermost shell in the high-speed region, which exceeds the contribution from the outermost shell by more than an order of magnitude.

Figure 3 demonstrates that the relative Barkas splitting in the outermost shell of Al is smaller than in the other shells over the entire energy range covered in the graph. Above ∼1 MeV, the difference to the effect in the innermost shell amounts to two orders of magnitude. As was to be expected from figure 2, the Barkas splitting of the M shell approximates the Barkas splitting of an Al atom very well up to almost 0.1 MeV/u, but already at 0.2 MeV/u it underestimates the effect for an Al atom by more than a factor of two.

This point is relevant to a recent study by Archubi et al. [18], where Barkas splittings are reported for He, Li, Ne and Ar ions in aluminium. Calculations refer to the M shell only and lead to results quite similar to ours. However, K and L shell splittings were not considered, and it was inferred that computed M shell splittings represent the entire effect to be observed on an aluminium target. As an example, for He at 1 MeV/u, the quoted Barkas ratio is 0.011, corresponding to ~ 0.005 for hydrogen ions, while our figure 3 delivers a value of 0.053, i.e., an order of magnitude higher.

For practical purposes, stopping cross sections are of more interest than relative Barkas splittings, an experimental determination of which would require systematic stopping measurements on a series of more or less stripped aluminium ions. Figure 4 shows what happens if a Barkas-Andersen correction is only applied to the M shell, as was done in ref. [18]. The upper graph indicates an error of $\sim$ 10 % in a broad regime around the stopping maximum. This is outside experimental error for the best experiments, although not for all [38]. The lower graph shows

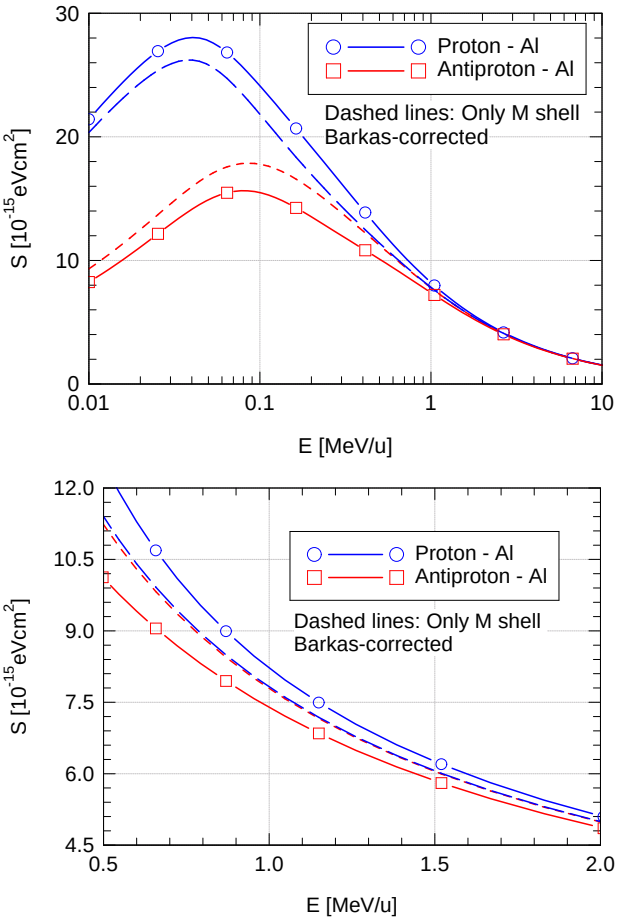

Fig. 4. Stopping cross sections for protons and antiprotons in aluminium from binary stopping theory. Solid lines: Full Barkas-Andersen included. Dashed lines: Only the outermost shell incorporate a Barkas-Andersen correction. The lower graph isolates the behavior between 0.5 and 2 MeV.

that at energies above 0.5 MeV, where precision data with an accuracy of $\sim$ 1 % exist ([39, 40] and numerous followup papers by the two groups), such an estimate causes an error of $\sim$ 3–5 %, which is far outside experimental error. As a matter of fact, the coincidence of the two dashed curves in the lower graph shows that such an estimate would not predict a noticeable Barkas splitting. After all, this is the regime where Andersen's original observations were made [4], and it is an important regime in ion beam analysis, a key area for the application of precision data on stopping.

We note that reported results refer to protons and antiprotons. Screening by projectile electrons, which is relevant for measurements with protons, will be considered in the following section. The point is not relevant for antiprotons.

This discussion adds another point to the second question asked in the introduction. Considering the fact that a free-electron description of the Barkas-Andersen effect in ordinary cold matter is relevant primarily for the outer shell of a metallic target, we may conclude that a char-

acterization of Barkas splitting in terms of a free-electron model – instructive as it may be as a model for academic study – requires great caution to avoid arriving at misleading results. Moreover, as is evident from figure 4, inner-shell effects are of central importance in practical applications of particle stopping.

6 Role of Screening

Originally, interest in the Barkas-Andersen effect arose in connection with the stopping of *point charges*, because both the Bethe stopping cross section and the Rutherford formula are independent of the sign of the charge.

Light ions tend to carry bound electrons at low beam velocities, and heavy ions carry electrons at all but the highest beam velocities. The potential of an ion surrounded by bound electrons is screened, and the stopping cross section of a screened Coulomb potential is not independent of the sign of the charge, as is evident from all results based on eq. (7). In other words, although a difference in stopping cross section between a dressed ion and an equivalently-dressed anti-ion may contain a Barkas-like component, it may be questioned whether this should be called a Barkas effect.

As a specific example, figure 5 shows stopping cross sections of aluminium for fully-stripped as well as neutral argon and antiargon ions. A neutral antiargon is an antiargon nucleus binding 18 positrons. Calculations have been performed by the PASS code (binary theory), and energy loss to projectile excitation has been ignored for clarity of the argument. As is to be expected, the stopping cross section for the neutrals is considerably smaller than for the bare ions. Curves for equilibrium ions, assuming the standard formula

$$\frac{q_1}{Z_1} = 1 - e^{-v/v_0 Z_1^{2/3}} \tag{20}$$

for the charge ratio q_1/Z_1 are also included to qualitatively indicate the region of significant screening. All ions experience splitting which is expressed by the Barkas ratio R, eq. (4) in the lower graph. The following observations may be made:

- Moving from high projectile speed downward, screening and Barkas splitting of the bare ions set in at ~ 1 MeV/u.
- For neutral ions, splitting sets in at ~ 100 MeV/u.
- This is to be expected, since the effective screening radius a is given by approximately [41]

$$\frac{1}{a^2} = \left(\frac{\omega}{v}\right)^2 + \frac{1}{a_{\rm sc}^2}, \tag{21}$$

  where $a_{\rm sc}$ characterizes the static screening of the electron cloud.

While penetrating neutral ions at 100 MeV/u are of rather academic interest, the calculated splitting at low energies is unquestionably real, and evident also in the curves labeled Ar^+ and Ar^-. The question may be asked, however,

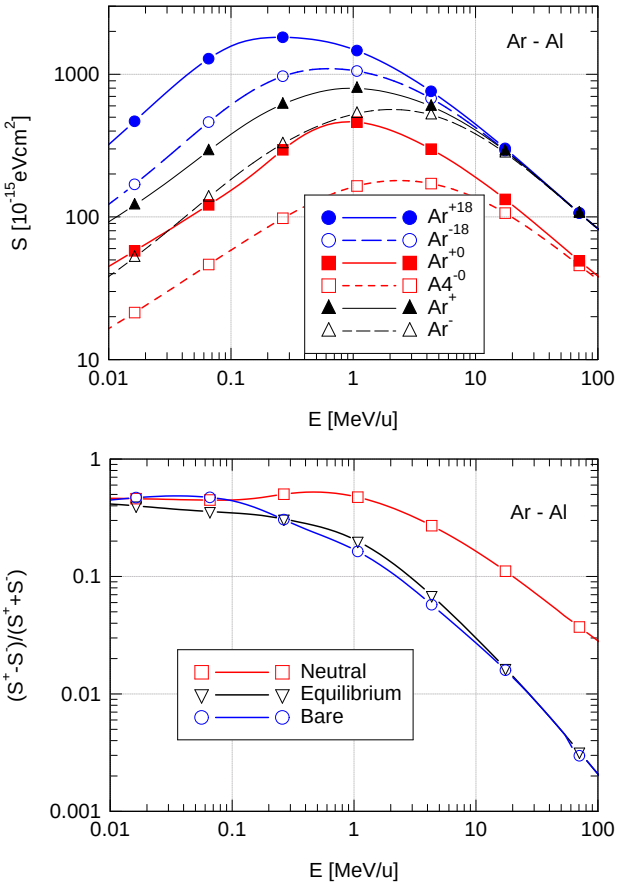

Fig. 5. Upper graph: Stopping cross sections of argon (solid lines) and antiargon (broken lines) in aluminium according to binary theory (PASS code). ±18: bare ions; ±0: neutral ions. ±: equilibrium charge. Projectile excitation ignored. Lower graph: Barkas ratio R.

whether this splitting, which is almost independent of the charge, should sort under Barkas splitting.

In general, inverting the sign of the interaction changes the scattering process and all cross sections. The differential cross section is invariant toward changing the sign in the perturbation limit (small-angle scattering) and, specifically, for Coulomb interaction.

In early experiments [5, 6], great care was taken to avoid drawing misleading conclusions from measurements involving Li ions with charge states below 3+. This was at a time when the main purpose of the measurements was to verify the existence of Z_1^3 and Z_1^4 corrections. At this point, it makes sense to talk about Barkas splitting and Barkas-Andersen corrections as long as the screening correction is small. Conversely, if the screening correction is large, S^+ and S^- are still meaningful concepts while S_0 and ΔS, eq. (3) and (2) are not.

Moreover, on the experimental side it is common to determine Barkas splitting by comparing the stopping of dressed hydrogen ions to the stopping of bare antiprotons [42]. Such measurements reveiled large differences. Although theory can provide estimates of either quantity, it is not meaningful to extract quantities S_0 and ΔS from

such measurements except in the regime of weak screening[2].

6.1 Electron-Ion Scattering

Recently, Grande & Vos [19] explored cross sections for elastic scattering of electrons from ions and neutral atoms with the specific purpose to explore the Barkas effect. Such measurements provide information about the screening potential of an ion in a given charge state in a way that is rather directly related to the quantity needed in a calculation of the stopping cross section of a free electron gas for a screened ion, namely via the differential scattering cross section.

While such measurements may provide useful input into calculations of the interaction of screened ions with matter, we find it misleading to categorize them under the heading of Barkas effect. After all, if one accepts that the nontrivial part of the Barkas-Andersen effect concerns bare ions, then these scattering measurements will just reproduce the Coulomb cross section.

There is an option to perform such measurements with positrons in addition to electrons. Scattering of positrons on a screened ion simulates scattering of electrons on a screened antiion. This may provide input into calculations of S^- for heavy screening.

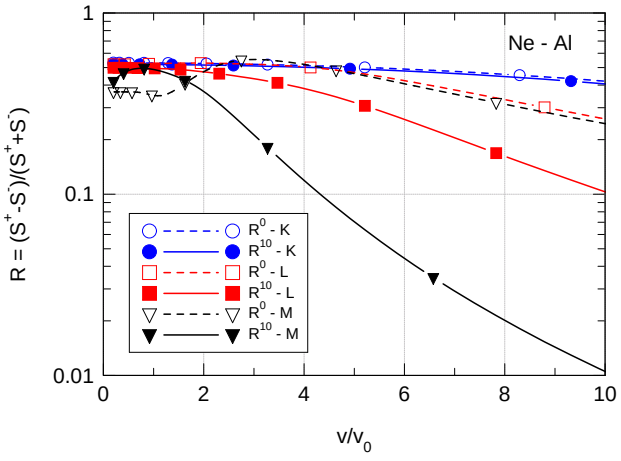

Fig. 6. Barkas Ratio R for Ne ions in Al according to PASS, separated into target shells.

In this connection it is interesting to compare the splitting for different shells. Figure 6 shows the case of Ne on Al. Pronounced Barkas splitting is seen for the Al-K shell, independent of the charge of the ion. For the M shell, the neutral ion shows strongly enhanced splitting as compared with the bare ion by more than a factor of two at the upper end of the velocity scale, and for the M shell the apparent Barkas splitting for the neutral exceeds the genuine Barkas splitting for the bare ion by more than an order of magnitude. Just as in the lower graph in figure 5, this large enhancement is not the least caused by a small denominator in eq. (1).

We do not want to deny by any means the relevance of electron scattering measurements to stopping theory, but we want to emphasize that these experiments do not address the main problem in the Barkas-Andersen effect. Note in particular that the effect of bound target electrons is not even considered. In the nomenclature of ref. [19], a penetrating point charge does not reveal a Barkas effect. Moreover, the theoretical considerations rest on the cross section for elastic scattering which ignores potential-energy transfer.

7 Discussion

Distinguishing between Barkas splitting and Barkas-Andersen correction, mentioned in the introduction to characterize the historical development, is also useful as a reference for what has been learned here. In brief, Barkas splitting characterizes the physics, and the Barkas-Andersen correction is an important ingredient of a stopping calculation. On the other hand, existing technology allows to measure Barkas splitting only for protons and antiprotons and other pairs of quasi-point charges. Measuring Barkas splitting for individual target shells is possible in principle, but such measurements have not been performed for any target material to our knowledge, and it is not obvious whether such measurements would provide information going beyond what can be extracted from existing theory.

After all, well-established theory predicts that Barkas splitting decreases in relative magnitude going from inner to outer target shells. This is obvious for a classical or quantal harmonic oscillator. For an electron-gas the same feature emerges in the local-density scheme via increased plasma frequency with increasing electron density. It is, therefore, misleading, as was done in ref. [18], to plot Barkas ratios for aluminium, evaluated on the basis of calculations for the M shell only.

Describing the Barkas-Andersen effect in terms of screening ties the effect to that of static screening by electrons bound to the projectile. So far, most often exponential screening has been assumed. If all asymmetry in the nuclear charge is ascribed to Barkas splitting, the magnitude of the effect tends to increase from bare to neutral ions. However, the physical meaning of a Barkas ratio, defined for a dressed ion by eq. (1), becomes unclear in case of dominating static screening: Neither the numerator nor the denominator can be measured by avaliable technology, and the average – which can be identified e.g. as the Bethe formula in the case of weak screening – has no a priori theoretical significance. As far as we can see, scaling laws for R of the type proposed in ref. [18] and [19] represent a property of Yukawa screening rather than Barkas splitting.

As far as the Barkas-Andersen correction in the stopping cross section is concerned, the close connection be-

[2] In our earlier study [22], calculated stopping cross sections for dressed heavy ions were compared to those for bare antiions via the ratio S^+/S^-. Equation (1) was not invoked.

tween the two types of screening just implies that both effects need to be applied to obtain a reliable estimate. This is the case for our PASS code [36], for the code of Arista [43], and for recent versions of the CasP code [44]. In equilibrium stopping, projectile screening tends to dominate over the Barkas-Andersen correction for heavy ions, as is seen in figure 5 upper part, and vice versa for low Z_1.

In connection with the measurements by Grande and Vos [19], we noted already that such measurements may indeed become of interest to stopping theory. However, accepting that these measurements determine the Barkas effect would imply that the only projectile that does not reveal a Barkas-Andersen effect is a point charge.

As concerns the questions posed in the introduction we conclude as follows:

- We find that Lindhard's approach to the Barkas-Andersen effect does extend into the distant-collision regime, although the agreement with the data by Ashley et al. is not perfect. Allowance for an equivalent of potential-energy transfer is important, however.
- As stated above, we find the analogy between the interaction of a swift ion and an atom and that with an electron gas to be about as close in the third as in the second order in Z_1.
- We recommend to reserve the terminology of Barkas splitting to bare or weakly-screened ions, where it is a nontrivial phenomenon.

This work has been supported by the Carlsberg Foundation.

References

1. F. M. Smith, W. Birnbaum and W. H. Barkas, Phys. Rev. 91 (1953) 765.
2. W. H. Barkas, W. Birnbaum and F. M. Smith, Phys. Rev. 101 (1956) 778.
3. W. H. Barkas, J. N. Dyer and H. H. Heckman, Phys. Rev. Lett. 11 (1963) 26.
4. H. H. Andersen, H. Simonsen and H. Sørensen, Nucl. Phys. A125 (1969) 171.
5. H. H. Andersen, J. F. Bak, H. Knudsen, P. Møller Petersen and B. R. Nielsen, Nucl. Instrum. Methods 140 (1977) 537.
6. H. H. Andersen, J. F. Bak, H. Knudsen and B. R. Nielsen, Phys. Rev. A 16 (1977) 1929.
7. L. H. Andersen, P. Hvelplund, H. Knudsen, S. P. Møller, J. O. P. Pedersen, E. Uggerhøj, K. Elsener and E. Morenzoni, Phys. Rev. Lett. 62 (1989) 1731.
8. R. Medenwaldt, S. P. Møller, E. Uggerhøj, T. Worm, P. Hvelplund, H. Knudsen, K. Elsener and E. Morenzoni, Nucl. Instrum. Methods B 58 (1991) 1.
9. R. Medenwaldt, S. P. Møller, E. Uggerhøj, T. Worm, P. Hvelplund, H. Knudsen, K. Elsener and E. Morenzoni, Physics Letters A 155 (1991) 155.
10. J. C. Ashley, R. H. Ritchie and W. Brandt, Phys. Rev. B 5 (1972) 2393.
11. P. Sigmund, *Particle penetration and radiation effects*, vol. 151 of *Springer Series in Solid-State Sciences* (Springer, Berlin, 2006).
12. H. Bethe, Ann. Physik 5 (1930) 324.
13. J. Lindhard, Nucl. Instrum. Methods 132 (1976) 1.
14. N. Bohr, Philos. Mag. 25 (1913) 10.
15. H. Esbensen, *Contributions to detailed perturbation theory for slowing-down of charged particles*, Ph.D. thesis, Aarhus University (1976).
16. K. W. Hill and E. Merzbacher, Phys. Rev. A 9 (1974) 156.
17. N. R. Arista, P. L. Grande and A. F. Lifschitz, Phys. Rev. A 70 (2004) 042902.
18. C. D. Archubi, I. Abril, R. Garcia-Molina and N. R. Arista, Nucl. Instrum. Methods B 316 (2013) 88.
19. P. L. Grande and M. Vos, Phys. Rev. A 88 (2013) 052901.
20. P. Sigmund and A. Schinner, Europ. Phys. J. D 12 (2000) 425.
21. M. Abramowitz and I. A. Stegun, *Handbook of mathematical functions* (Dover, New York, 1964).
22. P. Sigmund and A. Schinner, Nucl. Instrum. Methods B 212 (2003) 110 .
23. P. Sigmund and A. Schinner, Europ. Phys. J. D 15 (2001) 165.
24. C. Lehmann and G. Leibfried, Z. Physik 172 (1963) 465.
25. A. Schinner and P. Sigmund, Nucl. Instrum. Methods B 164-165 (2000) 220.
26. C. C. Sung and R. H. Ritchie, Phys. Rev. A 28 (1983) 674.
27. J. Lindhard, Mat. Fys. Medd. Dan. Vid. Selsk. 28 no. 8 (1954) 1.
28. J. Lindhard and A. Winther, Mat. Fys. Medd. Dan. Vid. Selsk. 34 no. 4 (1964) 1.
29. H. A. Kramers, Physica 13 (1947) 401.
30. N. R. Arista, Phys. Rev. A 26 (1982) 209.
31. N. R. Arista and P. Sigmund, Phys. Rev. A 76 (2007) 062902.
32. H. Esbensen and P. Sigmund, Ann. Physics N.Y. 201 (1990) 152.
33. C. D. Hu and E. Zaremba, Phys. Rev. B 37 (1988) 9268.
34. J. M. Pitarke, R. H. Ritchie and P. M. Echenique, Nucl. Instrum. Methods B 79 (1993) 209.
35. J. Pitarke, R. Ritchie, P. Echenique and E. Zaremba, Europhysics Letters 24 (1993) 613.
36. P. Sigmund and A. Schinner, Nucl. Instrum. Methods B 195 (2002) 64.
37. ICRU, *Stopping of ions heavier than helium*, vol. 73 of *ICRU Report* (Oxford University Press, Oxford, 2005).
38. H. Paul, *Stopping power graphs* (2013), URL `www.exphys.uni-linz.ac.at/stopping/`.
39. H. H. Andersen, A. F. Garfinkel, C. C. Hanke and H. Sørensen, Mat. Fys. Medd. Dan. Vid. Selsk. 35 no. 4 (1966) 1.
40. R. Ishiwari, N. Shiomi, S. Shirai and U. Uemura, Phys. Lett. A 48 (1974) 96.
41. P. Sigmund, Phys. Rev. A 56 (1997) 3781.
42. S. P. Møller, A. Csete, T. Ichioka, H. Knudsen, U. I. Uggerhøj and H. H. Andersen, Phys. Rev. Lett. 88 (2002) 193201.
43. N. R. Arista, Nucl. Instrum. Methods B 195 (2002) 91.
44. P. L. Grande and G. Schiwietz, *CasP version 5.2* (2013), URL `http://www.helmholtz-berlin.de/people/gregor-schiwietz/casp_en.html`.